JOURNAL OF CATALYSIS **169,** 85–92 (1997)
ARTICLE NO. CA971661

Density Functional Calculations of N_2 Adsorption and Dissociation on a Ru(0001) Surface

J. J. Mortensen,* Y. Morikawa,† B. Hammer,* and J. K. Nørskov*

*Center for Atomic-Scale Materials Physics (CAMP), Department of Physics, Technical University of Denmark, DK-2800 Lyngby, Denmark; and †Joint Research Center for Atom Technology (JRCAT), National Institute for Advanced Interdisciplinary Research (NAIR), 1-1-4 Higashi, Tsukuba, Ibaraki 305, Japan

Received December 20, 1996; revised February 7, 1997; accepted February 7, 1997

In order to understand the ammonia synthesis reaction over Ru-based catalysts, we have performed a series of density functional calculations of the adsorption and dissociation of N_2 on Ru(0001). We find molecularly and atomically adsorbed states of N_2 on Ru(0001) with structures, binding energies, and vibrational frequencies in good agreement with experimental data for these systems. We explain on the basis of the electronic structure of the Ru surface, the large difference in adsorption energy of N atoms in the hcp and fcc sites, the large diffusion barrier, and the large indirect N–N repulsion. The reaction path is determined using the hyperplane adaptive constraint method. We find that the lowest energy path shows a sizable barrier toward dissociation of 130 kJ/mol. During dissociation, the molecule, which is standing perpendicular to the surface in the molecularly adsorbed state, is first rotated into a metastable, flat-lying molecular precursor and is then dissociated into two adjacent hcp adsorption sites. We discuss the electronic structure along the reaction path and show that the N_2 induced dipole moment varies substantially. The variation of the dipole moment is used to discuss a possible model of the promoting effect of Cs on this reaction.

1. INTRODUCTION

The ammonia synthesis over Fe-based catalysts has been extensively studied for several decades (1). The reaction has also been studied over other metals (2), and recently a number of experimental studies of ammonia synthesis over Ru-based catalysts have appeared (3, 4). Just like for the Fe system, these studies have been augmented by studies of N_2 adsorption and dissociation on Ru single crystals (5, 6). The picture that emerges is that the N_2 dissociation step is rate limiting like on Fe. It also appears that alkali metals are strong promoters of the reaction on Ru, particularly Cs. The main difference from the Fe system is that the N_2 dissociation is considerably slower; the sticking probability is less than 10^{-12} at 300 K, compared to 10^{-6} on Fe(111) (5). Molecular beam scattering experiments have shown the direct dissociation of incoming N_2 molecules on Ru(0001) to be strongly activated, and that vibrational excitation of the incoming N_2 molecules is very effective in promoting the reaction (6). The same conclusion has been drawn from molecular beam scattering experiments on Fe(111) (7), but for this system it has been suggested that while molecules with a high kinetic energy dissociate directly upon impact and over a high barrier, the thermal process goes over a molecular precursor and is essentially nonactivated (8, 9). Similarly, it cannot be excluded that another, less activated dissociation channel exists on Ru. Another open question for the N_2/Ru system is that while alkali metals are strong promoters of the reaction (3, 4), the interaction between adsorbed N_2 and adsorbed alkali atoms is *repulsive* (10). This is completely the opposite of the Fe system, where the attractive interaction between N_2 and adsorbed alkali atoms is thought to be related to the promoting effect (8, 11).

To understand in more detail the ammonia synthesis reaction over Ru we have performed detailed density functional calculations of the reaction path for N_2 adsorption and dissociation over the Ru(0001) surface. Very recently calculations based on density functional theory (DFT) and with a nonlocal approximation to treat exchange and correlation effects (12) have proven able to treat large and complex systems of relevance for reactions on metal surfaces. Atomic and molecular bond energies and geometries as well as activation energies for simple surface reactions have been calculated (13–19) in good agreement with experimental results, where available. The calculations presented in the present paper show that the dissociation of N_2 is highly activated on Ru(0001), the minimum barrier being 1.36 ± 0.1 eV (130 kJ/mol). There are two molecularly adsorbed states, one chemisorbed species with the N–N axis perpendicular to the surface and another state which is lying flat on the surface and which is metastable. In the final state the chemisorbed N atoms are bound by 1.54 eV (150 kJ/mol N_2) and we find a strong N–N repulsion for coverages larger than a quarter of a monolayer. We use the calculated potential energy surface and the detailed information of the electronic structure of the system along the reaction path

0021-9517/97 $25.00

to discuss the reaction mechanism, including the possible effect of alkali promoters on this reaction.

In the following we first describe the calculational method in some detail. We then present our results for molecular and atomic chemisorption of N_2 and N on Ru(0001). Here there are extensive experiments to compare to and we use this system to illustrate the accuracy of the calculational approach. We then go on to present the potential energy surface for the dissociation process, and finally we discuss the implications of these results for the dynamics and kinetics of the dissociation process.

2. CALCULATIONAL METHOD

The calculation has two components. The first is the solution of the electronic structure problem and calculation of the total energy of the system at a fixed set of coordinates for all the atoms in the system. This is done using density functional theory. The calculation is *ab initio* in the sense that only the coordinates and nuclear charges are input into the calculations. The calculation has some approximations in terms of a finite size of the system treated, approximations for the exchange and correlation energy, and the use of pseudopotentials. These are all well tested, and we will also test the accuracy of the calculation below.

The Ru surface is modeled by a periodic array of slabs. Each slab is six atomic layers thick and there is a vacuum region between slabs of length 10.9 Å, corresponding to five Ru layers. The surface unit cell is a 2×2 unit cell as shown in Fig. 1. The use of a slab geometry instead of a cluster to describe the metal ensures that the metallic properties of the substrate are well described. Nitrogen is adsorbed only on one side, and the atoms in the first two Ru layers are allowed to relax. The difference in work function between the two slab surfaces is corrected for by adding a dipole layer of appropriate magnitude in the middle of the five vacuum layers.

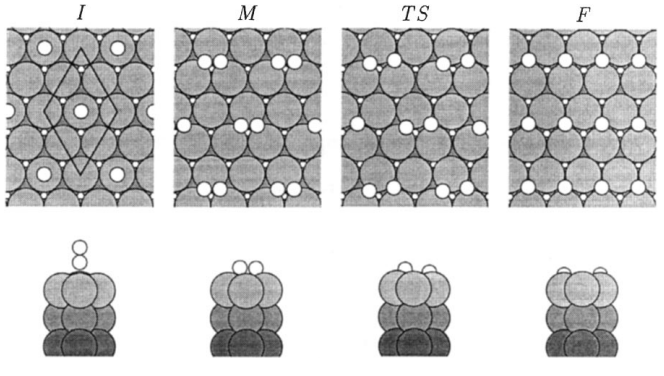

FIG. 1. Illustration of the unit cell used in the calculation and the configurations along the reaction path for N_2 dissociating over Ru(0001): (I) the initial, molecularly adsorbed state; (M) the metastable molecularly adsorbed state; (TS) the transition state; and (F) the final, dissociated state.

We use the generalized gradient approximation (12) (GGA) for the exchange and correlation energy and do fully selfconsistent pseudopotential calculations (12, 20). With these approximations, and the c/a ratio fixed at the experimental value (1.582), we get a lattice constant for bulk Ru of 2.757 Å, which is a few percent larger than the experimental value. This theoretical lattice constant is used in the slab calculations. In these calculations the pseudowavefunctions are expanded in plane waves with a cutoff of 40 Ry, and the surface Brillouin zone is sampled at 18 special **k**-points. In order to stabilize the numerical procedures, the occupation numbers are Fermi distributed with an electronic temperature of $kT = 0.05$ eV, and all total energies are extrapolated to $T = 0$ K. For details of the calculations we refer to Refs. (21) and (22).

The other part of the calculation is the determination of the minimum energy reaction path. Any chemical reaction can be viewed as a transition from one minimum (the reactants) to another (the products) on the potential energy surface describing the energy of all the atoms in the system as a function of their coordinates. In the following we denote a point in this configuration space by a vector containing all the coordinates of the M atoms in the system

$$\mathbf{\Gamma} = (\mathbf{R}_1, \mathbf{R}_2, \ldots, \mathbf{R}_M) \quad [1]$$

$$= (x_1, y_1, z_1, x_2, y_2, z_2, \ldots, x_M, y_M, z_M). \quad [2]$$

The minimum energy path is the most probable reaction path. It crosses between the two local minima over the lowest barrier, and this barrier will be the activation energy for the process. All other points along the minimum energy path are also the lowest energy point in all degrees of freedom except the one along the path. It is in general difficult to define algorithms that find the lowest energy path (23). The energy must be minimized relaxing all coordinates of the problem except one, the local direction of the path. Here we use the newly suggested method, the *hyper-plane adaptive constraint* (HAC) method (24), which can be viewed as a simplified version of the Nudged Elastic Band method of Mills *et al.* (23).

In the HAC method an initial guess at a path is first made. We use a linear interpolation between the initial and the final state ($\mathbf{\Gamma}_I$ and $\mathbf{\Gamma}_F$). We illustrate this in two dimensions in Fig. 2. The figure shows the (z, b) plane spanned by the height z of the N_2 molecule above the Ru surface and the N–N bond length b. The two end points represent the molecularly adsorbed state of N_2 (I) and the atomically chemisorbed state (F), which is closer to the surface and has a much longer N–N bond length. The line connecting these two points is the starting guess. We point out that in the full calculations we consider not only the (z, b) plane but all six N_2 coordinates and all the coordinates of the Ru atoms in the first two layers of the surface.

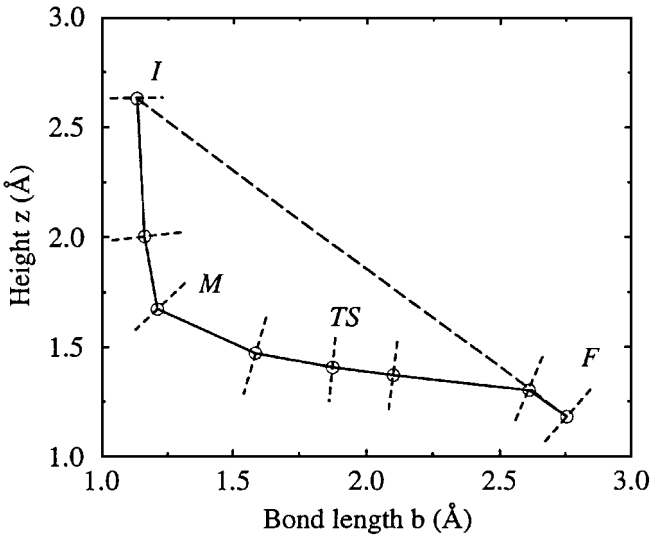

FIG. 2. Illustration of the hyper-plane adaptive constraint (HAC) method for finding the minimum energy reaction path. The figure shows the initial guess and the final path for N_2 dissociation on Ru(0001) in the (z, b) plane spanned by the height z of the center of mass of the molecule over the Ru surface plane and the N–N bond length b. The initial guess is just the dashed line connecting the initial (I) and final (F) state. After minimizing the energy perpendicular to the local path the minimum energy path, shown as a solid line, develops. The constraint is defined along the way as the hyperplane perpendicular to the line connecting the two neighboring points on the path. The hyperplanes for the final path are sketched at the images used.

One should note that the path found with the HAC method will depend slightly on the choice of coordinates. However, stationary points along the path, such as the transition state, are independent of such choices.

In the implementation of the method only a finite number of points (images) along the path are considered. The coordinates of each image are first relaxed toward lower energy within the hyper-plane normal to the path. This is achieved by moving the point only along the force perpendicular to the path. Often it is necessary to add extra images along the path—this can be done at any time of the calculation.

To ensure that the correct path is found, the hyper-plane constraints must be updated as the path changes. In general, the normal to the hyper-plane of image number n is defined as the vector $\mathbf{\Gamma}_{n+1} - \mathbf{\Gamma}_{n-1}$. This means that the constraint is modified under the influence of the motion of the rest of the path.

The final result is seen in Fig. 2 to be quite different from the initial guess. It can also be seen that the final constraints (shown dashed) are not perpendicular to the initial guess for the path. In fact, the method is quite robust even for complex paths, where simple intuitive approaches fail (25).

It is often useful to define a reaction coordinate s as the norm of the total change in all coordinates along the path, starting at the initial state $\mathbf{\Gamma}_I$:

$$s = \int_{\mathbf{\Gamma}_I}^{\mathbf{\Gamma}} |d\mathbf{\Gamma}|. \qquad [3]$$

For a finite number of images we use a discrete version of Eq. [3]:

$$s_n = \sum_{i=1}^{n-1} |\mathbf{\Gamma}_{i+1} - \mathbf{\Gamma}_i|. \qquad [4]$$

We stress here that the method is unbiased—only knowledge of the initial and final states of the reaction is input to the calculation. Other virtues are that only one constraint is imposed during relaxation and that relaxations of the substrate are easily included.

3. MOLECULAR AND ATOMIC CHEMISORPTION

We first consider the simple cases of atomic and molecular adsorption of N_2 on the Ru(0001) surface. In Table 1 we compare calculated and measured properties of gas phase N_2, molecularly chemisorbed N_2 and atomically chemisorbed N.

TABLE 1

Comparison of Calculated and Experimental Properties of Gas-Phase N_2 and Molecularly and Atomically Chemisorbed Nitrogen on Ru(0001)

	DFT	Exp.
Gas-phase N_2		
Bond length (Å)	1.11	1.10[a]
Frequency (cm^{-1})	2413	2359[a]
$(\sqrt{3}\times\sqrt{3})$R30°-N_2/Ru ($\theta = 1/3$)		
N–N bond length (Å)	1.13	1.10 ± 0.04[b]
Ru–N bond length (Å)	2.00	2.00 ± 0.05[b]
Buckling (Å)	0.15	0.00 ± 0.05[b]
N–N frequency (cm^{-1})	2239	2195[c]
Adsorption energy (eV/molecule)	−0.61	−0.44[d]
$p(2\times2)$-N_2/Ru ($\theta = 1/4$)		
Adsorption energy (eV/molecule)	−0.47	
$p(2\times2)$-N/Ru ($\theta = 1/4$)		
Ru–N bond length (Å)	1.98	1.93 ± 0.05[e]
Buckling (Å)	0.10	0.07 ± 0.04[e]
N(⊥)-frequency (cm^{-1})	534	573[f]
N(=)-frequency (cm^{-1})	507	
Adsorption energy (eV/atom)	−0.77	
Adsorption energy (fcc site) (eV/atom)	0.00	
Diffusion barrier (eV)	0.93	0.94 ± 0.15[g]
$c(2\times2)$-N/Ru ($\theta = 1/2$)		
Adsorption energy (hcp sites) (eV/atom)	−0.19	

Note. The chemisorbed N atoms are positioned in hcp sites unless otherwise stated. All adsorption energies are relative to gas phase N_2. The buckling is the lifting of the Ru atoms under the molecule relative to its nearest neighbors in the surface layer. The theoretical results in the $(\sqrt{3}\times\sqrt{3})$R30° structure are from Ref. (26). The experimental data are from: [a]Ref. (27); [b]Ref. (28); [c]Ref. (10); [d]Ref. (29); [e]Ref. (30); [f]Ref. (31); [g]Ref. (32).

The calculations have been done by placing the adsorbate in a certain site and varying all degrees of freedom of the adsorbate and the two first layers of Ru, to find the most stable adsorption site. This defines the adsorption energy (with no zero point energies for vibrations included) and the adsorption geometry. From small variations in the adsorbate position around the minimum energy position we get the second derivatives of the energy and hence the vibrational frequencies.

For the molecularly adsorbed state we have considered both a (2×2) and a $(\sqrt{3} \times \sqrt{3})$R30° unit cell, because experimentally, adsorbed N_2 is known to order in a $(\sqrt{3} \times \sqrt{3})$R30° structure (5, 10). The details of the $(\sqrt{3} \times \sqrt{3})$R30° calculation can be found in Ref. (26). It is seen in Table 1 that the calculation also favors the $(\sqrt{3} \times \sqrt{3})$R30° structure for the molecularly adsorbed state. The adsorption structure is shown in Fig. 1 (the initial state I) for the (2×2) structure. The vibrational frequency of N_2 is also reasonably described, and in particular the shift of 174 cm^{-1} in the frequency upon adsorption compares very well with the experimentally observed shift of 164 cm^{-1} (29). The difference between the experimental and calculated chemisorption energy of N_2 of about 0.2 eV sets the scale of the absolute accuracy of the calculated energies.

As shown in Ref. (26) the electronic structure of chemisorbed N_2 can be understood qualitatively and semiquantitatively in terms of an interaction between the molecular 5σ and $2\pi^*$ states and the metal *d* states.

We further show in Table 1 that the present calculational method accurately describes the properties of atomically adsorbed N for the $p(2 \times 2)$ structure where comparison to experiment can be done. The N atom sits threefold coordinated in an hcp site as shown in Fig. 1 (F) for the hypothetical $c(2 \times 2)$ geometry. The chemisorption energy is predicted to be 2×0.77 eV $= 1.54$ eV (~150 kJ/mol) per N_2 molecule in the most stable $p(2 \times 2)$ structure at a quarter of a monolayer coverage. At higher coverages where the N atoms "share" Ru atoms the chemisorption energy drops to 2×0.19 eV $= 0.38$ eV (~40 kJ/mol). There is thus a sizable N–N repulsion above a quarter of a monolayer coverage. The structure and energetics of atomic chemisorption agree well with the calculations of Schwegmann *et al.* (30).

The DFT result for the barrier for diffusion of atomic N is 0.93 ± 0.1 eV which is in good agreement with a recent experiment showing the barrier to be 0.94 ± 0.15 eV (32). It should be noted that there is a large difference in energy between the equilibrium hcp site for adsorption and the fcc site of 0.77 eV—this preference for the hcp site is also found experimentally (32).

The difference in N adsorption energy in hcp, fcc, and bridge sites as well as the effect of preadsorbed N atoms can all be traced back to differences in the coupling between the N2*p* states and the Ru *d* bands. This coupling is illustrated in Fig. 3. We suggest that it is most convenient to consider first

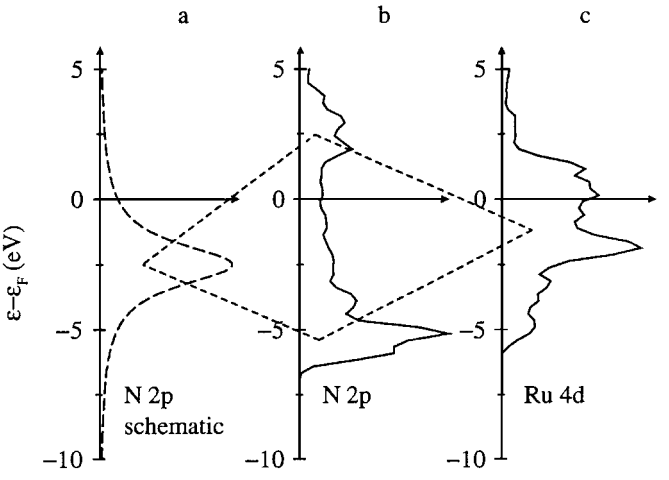

FIG. 3. Illustration of the coupling of the renormalized N2*p* state to the Ru *d* band. (a) Schematic of the N2*p* state after coupling to the *sp* electrons of the substrate. (b) Self-consistently calculated DOS projected onto the 2*p* orbitals of N atom adsorbed in an hcp site. (c) Self-consistently calculated Ru *d* DOS for the clean surface.

the coupling between the adsorbate states and the metal *sp* electrons and then include the effect of the coupling to the *d* electrons (13, 33–35). The former gives rise to a shift and broadening of the adsorbate levels, while the latter gives rise to the formation of bonding states below the *d* bands and antibonding states above.

The coupling to the metal *sp* electrons varies much less from one metal to another or from one site to another than the *d*-coupling. We can therefore ascribe the variations in adsorption energy directly to variations in the *d* density of states (DOS). Figure 4 shows comparisons of the calculated

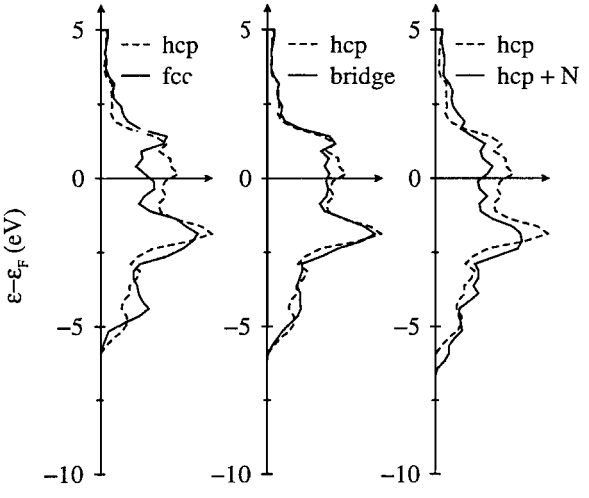

FIG. 4. Density of states projected onto Ru d_{z^2} orbitals pointing toward different adsorption sites for N atoms. The four different sites are hcp, fcc, bridge, and an hcp site where the Ru atom has an N atom adsorbed in a neighboring hcp site.

DOS of the clean surface projected onto a Ru d_{z^2} orbital pointing toward the N adsorption site above an hcp, an fcc, and a bridge site (the z-axis is directed from the center of the Fe atom to the center of the N atom). We also show the DOS toward an hcp site for a Ru atom which already has one N nearest neighbor (calculated for the $p(2 \times 2)$ structure). The d-DOS at the fcc site can be seen to be broader than that at the hcp site. This signifies that the d states pointing in this direction bond strongly to the Ru atoms in the second layer, leading to bonding and antibonding Ru–Ru states. The deep lying d states cannot be shifted through the Fermi level due to the interaction with the adsorbate states, and therefore do not contribute as much to the bonding of the adsorbate to the surface. The same effect is seen for the Ru d-states that have already interacted with a N atom. The bridge site DOS looks much more like the hcp one, but here only two N2p states can couple strongly to the Ru d states instead of three in the hcp (or fcc) site.

We can substantiate that it is the difference in the d-DOS that determines the variations in the N chemisorption energy by using the Newns–Anderson model (36) to directly link the adsorption energy to changes in the d-DOS of the metal atoms to which the N atom couples. We use the same parameters as for O2p for the coupling matrix element (35) and a position of the N2p states 2.5 eV below the Fermi level (see Fig. 3). The N–Ru distance is so that in the threefold (fcc or hcp) sites each of the three 2p orbitals interacts with one "directed" d orbital on each of the three Ru neighbors (37), and in the twofold site only two 2p states are assumed to interact. This gives a difference between fcc and hcp of 0.62 eV (to be compared to the full DFT–GGA result of 0.77 eV from Table 1), a difference between bridge and hcp of 1.12 eV (to be compared to the full DFT–GGA result of 0.93 eV from Table 1), and a difference in binding energy per N atom between the $p(2 \times 2)$ and $c(2 \times 2)$ structures of 0.45 eV (to be compared to the full DFT–GGA result of 0.58 eV from Table 1).

From the above simple modeling, it can be seen that the coupling of N2p states to the d band of a Ru atom modified by a neighboring N atom, can account for the main part of the N–N repulsion. The N–N (indirect) interaction can therefore be understood in a sequential adsorption model, in the following way: First one N atom is adsorbed. This modifies (shifts down) the d states of the neighboring Ru atoms. The next N atom will see a modified d band and bind weaker than the first. It is clear that only two N atoms that bond to the same Ru atom will experience a N–N repulsion in this picture. The repulsion can therefore be viewed as due to the "sharing" of the metal atoms.

4. THE DISSOCIATION PATH

We now turn to the dissociation reaction. We use the HAC method described above to get the minimum energy reaction path connecting the adsorbed molecular state and the dissociated state. The energy as a function of the reaction coordinate, Eq. [4], is shown in Fig. 5. To plot a smooth curve through the points we have also used the first derivatives $dE/ds = -\mathbf{F} \cdot d\mathbf{\Gamma}(s)/ds$, where $\mathbf{F}$ is the force. Also shown in Fig. 5 are the variations in selected coordinates along this path. It can be seen that the height of the molecule above the first Ru layer decreases monotonically along the reaction path. The N–N bond length stays almost constant for the first part of the reaction, where the molecule rotates.

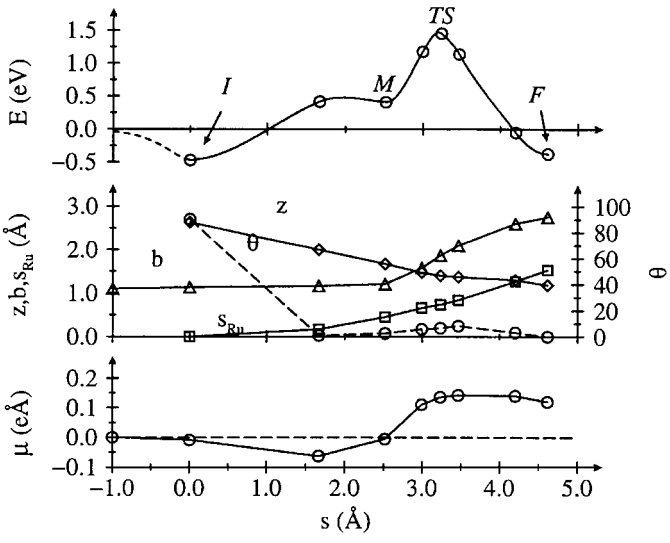

FIG. 5. (Top) The calculated energy (E) along the reaction path for N_2 dissociating over a Ru(0001) surface. The forces parallel to the reaction path have been used in constructing the fit. (Middle) The variation of the height of the molecular center of mass above the Ru surface layer (z), the N–N distance (b) and the angle of the N–N bond axis with respect to the surface plane (θ). To illustrate the degree of substrate relaxations along the reaction path, the contribution of the Ru degrees of freedom to the reaction coordinate is also shown (s_{Ru}). (Bottom) The N_2-induced dipole moment (μ) along the reaction coordinate.

The picture that emerges from Fig. 5 is the following. As the molecule approaches the surface it is first attracted toward a molecularly adsorbed state (denoted I in Fig. 1). Here the molecule stands perpendicular to the surface, and has the properties discussed in the preceding section. Further along the reaction coordinate, the molecule rotates, and a new metastable molecularly adsorbed state is seen (M in Fig. 1). Continuing along the reaction coordinate, the energy continues to increase until the transition state (TS in Fig. 1). The transition state is characterized by a very stretched molecule. One of the N atoms is already close to the final state in the threefold hollow site, whereas the other is twofold coordinated to the Ru underneath. Finally, the two N atoms end up in hcp sites. The energy is still higher than the lowest energy state discussed in the preceding section, because the two N atoms still feel a repulsion from each other (they still "share" one Ru atom). Diffusion to

adjacent hcp sites will then lower the energy of the system from −0.38 to −1.54 eV (see Table 1).

Apart from the residual interaction between the two N atoms that have just dissociated from each other in the final state in Fig. 1 (F), it can be seen that due to computational limitations we have used a unit cell where the N atoms in adjacent unit cells also "share" Ru atoms in the final state of the reaction. Had the dissociation taken place at a lower coverage (in a larger unit cell), the energy in the final state would have been somewhere in between −0.38 and −1.54 eV. This does not mean that the finite size of the unit cell gives a similar error in the transition state. It can be seen in Fig. 1 (TS) that in the transition state no N atoms "share" any Ru atoms through the periodic boundary conditions, so the interactions will be substantially weaker here. In order to estimate the magnitude of these interactions, we have calculated the energy of the transition state in two different unit cells, a 2×2 and a 3×2. In these calculations the substrate is represented by only two Ru layers. The effect of increasing the unit cell size, and thereby increasing the distance between neighboring dissociating molecules, is a lowering of the barrier by 0.12 eV.

The DOS projected onto the two N atoms in the transition state are shown in Fig. 6. Because of the very stretched N–N bond length in the transition state (1.9 Å), the electronic structure of the molecule is very final state-like. The large splitting of the N2*p* states that is seen in the molecularly adsorbed state (I in Fig. 1) (26) is only small in the transition state. The 2*p* projected DOS on the two N atoms are both very similar to the DOS shown in Fig. 3b for a N atom adsorbed in an hcp site. The differences are due to the small residual N–N interaction and also due to the different Ru–N bond lengths.

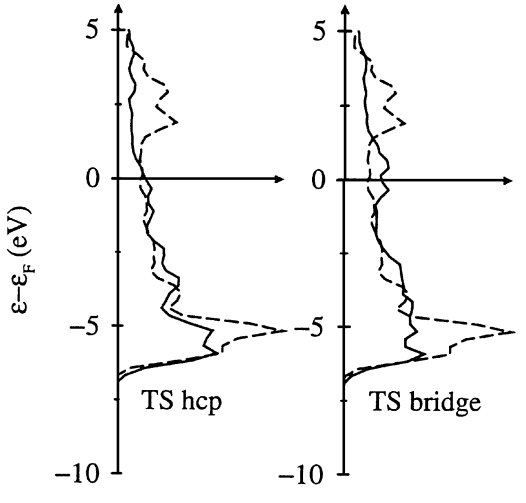

FIG. 6. DOS projected onto 2*p* orbitals of the two N atoms in the transition state. One atom is close to an hcp site and one is close to a bridge site. Both DOS are compared with the DOS projected onto the 2*p* orbitals of a N atom adsorped in an hcp site (shown dashed).

The contribution from the Ru degrees of freedom to the reaction coordinate, Eq. [4], is also shown in Fig. 5. It is seen that there is a substantial rearrangement of the substrate, particularly during the later parts of the reaction. This means that one cannot think of the surface as a passive substrate providing sites for adsorption. It takes a vital part in the dissociation process.

5. DISCUSSION

The calculated potential energy diagram in Fig. 5 provides a very nice explanation of the experimental observations regarding the dynamics and kinetics of the N_2 dissociation reaction on the Ru(0001) surface. It is seen that there is no nonactivated path. The top of the barrier is at 1.48 eV above the energy of the free molecule. Correcting for finite size effects, as estimated above, we find that all dissociating molecules must overcome a barrier of at least 1.36 eV. This first of all explains the extremely low dissociative sticking probability measured for this surface (5). The finding of a large barrier in Fig. 5 is in good qualitative agreement with molecular beam experiments (6).

The barrier for rotating the N_2 molecule into the metastable molecularly adsorbed state is 0.5 eV. The barrier for the molecule to desorb or rotate back to the initial state is small, but this state might still play a role as a mobile precursor at synthesis conditions. In spite of the short lifetime of this state, the molecule will have the possibility of moving around on the surface in this state for a limited time to find sites (defects or promoters) where dissociation is facile.

It might be possible to detect signatures of the down lying molecular state (M) during desorption. Desorbing molecules might exchange energy with the substrate after having surmounted the transition state. This would mean that the desorbing molecules would not have a kinetic energy corresponding to the full potential energy (the barrier height) at the transition state. There have been indications of such an effect in experiments monitoring the angular distribution of desorbing N_2 (38). A clarification of the effect of this state on the dynamics and kinetics of the dissociation process will have to await a more detailed simulation of the dynamics and more detailed experiments.

One of the open questions in connection with the Ru catalyst for ammonia synthesis is the role of coadsorbed alkalis. It is well established that alkali metals promote the reaction considerably (2–4). The state of Cs on the surface may be associated with co-adsorbed oxygen (39), but irrespective of the detailed structure of the Cs on the surface it is tempting to suggest that the effect of the Cs is the same as the effect of K on Fe catalysts, that is, to stabilize N_2 on the surface and lower the barrier for N_2 dissociation (8, 11). Such a stabilization has been explained in terms of the electrostatic interaction between the adsorbed N_2 and K

(40, 41): Adsorbed N_2 on Fe(111) (the α state) gives rise to an increased workfunction corresponding to electron transfer from the surface toward the molecule, while adsorbed K gives rise to a dipole with the opposite orientation (if the K is associated with adsorbed oxygen, this dipole is typically even larger). This gives an attractive interaction, and estimates of the dipole moments show that even the size of the effect is reasonable. This picture cannot be directly transferred to the case of N_2 on Ru(0001). Experiments show that the molecularly adsorbed N_2 *lowers* the work function and interacts repulsively with adsorbed K. This agrees with the electrostatic picture of the adsorbate-adsorbate interaction, but cannot explain the promoting effect of Cs on the synthesis reaction.

The key to this puzzle is perhaps found by considering the variation in the N_2-induced dipole moment along the reaction path in Fig. 5. It can be seen that the molecularly adsorbed state of the molecule does indeed give rise to a small decrease in the work function and thus to a small negative dipole moment. This will interact repulsively with the negative dipole moment of adsorbed K or Cs. Further along the reaction path, the dipole moment changes sign, and around the transition state it is large and positive. Any adsorbate that will give rise to a lowering of the work function of the surface will therefore lower the barrier due to electrostatic interactions.

Adsorption of Cs lowers the work function of Ru(0001) by up to 4 eV (42). The change in work function is a measure of the average change in electrostatic potential outside the surface due to adsorption of the alkali at a certain coverage. Since the typical length scale of such variations outside a metal surface is $\sim$1 Å (40, 41), this must mean that adsorbed Cs as optimum coverage gives rise to an electrostatic field of $\varepsilon \simeq 4$ V/Å. This value is an average parallel to the surface; some sites will experience a larger value, some sites a smaller one. Since the N_2 dipole moment at the top of the barrier is $\mu = 0.14$ eÅ, the first order lowering of the energy is $\delta E = \varepsilon\mu \simeq 4 \times 0.14$ eV $= 0.56$ eV (43). This will lower the barrier for dissociation almost to the level of the initial barrier for rotation of the molecule. The barrier for rotation will be slightly increased, because here the induced dipole moment has the opposite sign, but there is the possibility that the rotation takes place far from a promoter, and the metastable molecule migrates to the Cs atoms where they dissociate very fast.

The kinetic modeling of the ammonia synthesis reaction over Cs promoted Ru, has suggested a barrier of 33 kJ/mol for the dissociation step (4). This is in quite reasonable agreement with the barrier for the first rotation step in the calculations. It must, however, be stressed that the discussion above of the effect of Cs is only tentative.

We conclude that the density functional calculations give an excellent description of the atomic and molecularly adsorbed state of nitrogen on Ru(0001). The calculations also shed new light on the dissociation process—there are only highly activated reaction paths and there is a molecular precursor. Calculations of the nitrogen-induced dipole moment along the reaction path provides a possible explanation of the promoting effect of Cs and other alkali metals on the reaction.

ACKNOWLEDGMENTS

JRCAT is supported by the New Energy and Industrial Technology Development Organization (NEDO) of Japan. The present work was in part financed by The Center for Surface Reactivity under the Danish Research Councils and Grant 9501775. Center for Atomic-Scale Materials Physics is sponsored by the Danish National Research Foundation.

REFERENCES

1. "Topics in Catalysis. Frontiers in Catalysis: Ammonia Synthesis and Beyond" (H. Topsøe, M. Boudart, and J. K. Nørskov, Eds.), Vol. 1. Baltzer, Basel, 1994.
2. Ozaki, A., and Aika, K., *in* "Catalysis: Science and Technology" (J. R. Anderson and M. Boudart, Eds.), Vol. 1. Springer-Verlag, Berlin, 1981.
3. Tennison, S. R., *in* "Catalytic Ammonia Synthesis" (J. R. Jennings, Ed.), p. 303. Plenum, New York, 1991.
4. Hinrichsen, O., Rosowski, F., Muhler, M., and Ertl, G., *Chem. Eng. Sci.* **51**, 1683 (1996).
5. Dietrich, H., Geng, P., Jacobi, K., and Ertl, G., *J. Chem. Phys.* **104**, 375 (1996).
6. Romm, L., Katz, G., Kosloff, R., and Asscher, M., unpublished.
7. Rettner, C. T., and Stein, H., *Phys. Rev. Lett.* **59**, 2768 (1987).
8. Ertl, G., *Catal. Rev.-Sci. Eng.* **21**, 201 (1980).
9. Alstrup, I., Chorkendorff, I., and Ullmann, S., *Z. Phys. Chem.* **198**, 123 (1997).
10. de Paola, R. A., Hoffmann, F. M., Heskett, D., and Plummer, E. W., *Phys. Rev. B* **35**, 4236 (1987).
11. Stoltze, P., and Nørskov, J. K., *J. Catal.* **110**, 1 (1988).
12. Perdew, J. P., Chevary, J. A., Vosko, S. H., Jackson, K. A., Pederson, M. R., Singh, D. J., and Fiolhais, C., *Phys. Rev. B* **46**, 6671 (1992).
13. Hammer, B., and Nørskov, J. K., *Nature* **376**, 238 (1995).
14. Hammer, B., Morikawa, Y., and Nørskov, J. K., *Phys. Rev. Lett.* **76**, 2141 (1996).
15. Holmblad, M., Larsen, J. H., Chorkendorff, I., Nielsen, L. P., Besenbacher, F., Stensgård, I., Lægsgaard, E., Kratzer, P., Hammer, B., and Nørskov, J. K., *Catal. Lett.* **40**, 131 (1996).
16. Wilke, S., and Scheffler, M., *Phys. Rev. B* **53**, 4926 (1996).
17. White, J. A., Bird, D. M., and Payne, M. C., *Phys. Rev. B* **53**, 1667 (1996).
18. Wiesenekker, G., Kroes, G. J., Baerends, E. J., and Mowrey, R. C., *J. Chem. Phys.* **102**, 3873 (1995); ibid **103**, 5168 (1995).
19. Santen, R. A. V., and Neurock, M., *Catal. Rev. Sci. Eng.* **37**, 557 (1995).
20. White, J. A., and Bird, D. M., *Phys. Rev. B* **50**, 4954 (1994).
21. Kresse, G., and Furthmüller, J., *Comput. Mat. Sci.* **6**, 15 (1996).
22. Hammer, B., and Nielsen, O. H., *in* "Workshop on Applied Parallel Computing in Physics, Chemistry and Engineering Science" (J. Wasniewski, Ed.), Vol. 1041. Springer Lecture Notes in Computer Science, 1995.
23. Mills, G., Jónsson, H., and Schenter, G. K., *Surf. Sci.* **324**, 305 (1995).
24. Morikawa, Y., Mortensen, J. J., Jónsson, H., Hammer, B., and Nørskov, J. K., unpublished.
25. Jónsson, H., private communication.
26. Mortensen, J. J., Morikawa, Y., Hammer, B., and Nørskov, J. K., *Z. Phys. Chem.* **198**, 113 (1997).

27. Huber, K. P., and Herzberg, G., "Molecular Spectra and Molecular Structure. Constants of Diatomic Molecules." Vol. IV. Van Nostrand Reinhold, New York, 1979.
28. Bludau, H., Gierer, M., Over, H., and Ertl, G., *Chem. Phys. Lett.* **219**, 452 (1994).
29. Menzel, D., Pfnür, H., and Feulner, P., *Surf. Sci.* **126**, 374 (1983).
30. Schwegmann, S., Seitsonen, A. P., Dietrich, H., Bludau, H., Over, H., Jacobi, K., and Ertl, G., *Chem. Phys. Lett.* **264**, 680 (1997).
31. Shi, H., Jacobi, K., and Ertl, G., *J. Chem. Phys.* **99**, 9248 (1993).
32. Zambelli, T., Trost, J., Wintterlin, J., and Ertl, G., *Phys. Rev. Lett.* **76**, 795 (1996).
33. Holloway, S., Lundqvist, B. I., and Nørskov, J. K., *in* "Proceedings, 8th International Congress on Catalysis, Berlin, 1984," Vol. 4, p. 85. Dechema, Frankfurt-am-main, 1984.
34. Hammer, B., and Nørskov, J. K., *Surf. Sci.* **343**, 211 (1995).
35. Hammer, B., and Nørskov, J. K., *in* "Chemisorption and Reactivity on Supported Clusters and Thin Films" (R. M. Lambert, G. Pacchioni, Eds.), p. 285. Kluwer Academic Publishers, Dordrecht/Boston/London, 1997.
36. Newns, D. M., *Phys. Rev.* **178**, 1123 (1969).
37. Stokbro, K., and Baroni, S., *Surf. Sci.* **370**, 166 (1997).
38. Matsushima, T., *Surf. Sci.* **197**, L287 (1988).
39. Trost, J., Wintterlin, J., and Ertl, G., *Surf. Sci.* **329**, L583 (1995).
40. Nørskov, J. K., *in* "Physics and Chemistry of Alkali Metal Adsorption" (H. P. Bonzel, A. M. Bradshaw, and G. Ertl, Eds.), p. 253. Elsevier, Amsterdam/Oxford/New York/Tokyo, 1989.
41. Nørskov, J. K., Holloway, S., and Lang, N. D., *Surf. Sci.* **137**, 65 (1984).
42. Pirug, G., Ritke, C., and Bonzel, H. P., *Surf. Sci.* **257**, 50 (1991).
43. Hammer, B., Jacobsen, K. W., and Nørskov, J. K., *Surf. Sci.* **297**, L68 (1993).